

Earthquake Response Analysis of Multiple Towers on a Common Podium: A Representative Case Study

Cem TURA¹

Kutay ORAKÇAL²

ABSTRACT

In this study, a hypothetical tall building structure consisting of two towers and a common podium is analyzed, considering effects of interaction between the towers due to the connected podium floors. Interaction effects on the podium level are included in the analyses using either an upper bound or lower bound approach, by assigning fixed or free end restraints at the continuous boundaries of single tower models, respectively. Responses of the single tower models are then compared with the response obtained for the combined model, which includes both of the towers as well as the common podium and basements. Results obtained using different linear and nonlinear analysis methods indicate that single tower models with fixed end restraints overestimate the internal forces at the podium floors, although to a reasonable extent.

Keywords: Tall building, multiple towers, common podium, nonlinear analysis, performance based design.

1. INTRODUCTION

In projects with multiple towers on a common podium, even when the structural properties of the towers are similar to each other, dynamic response of the towers during real seismic events are likely to vary due to several reasons, including the service loads on the towers, local soil conditions, and spatial variability of the ground motion. Possible out of phase response of individual towers due to this variance in dynamic response may create excessive in-plane stresses at the connected podium level diaphragms. To prevent possible diaphragm failure, design engineers must consider these effects as critical (i.e., non-ductile) design quantities. Furthermore, such interaction between the towers may also influence the response

Note:

- This paper has been received on October 04, 2018 and accepted for publication by the Editorial Board on January 28, 2019.
- Discussions on this paper will be accepted by January 31, 2020.

• <https://dx.doi.org/10.18400/tekderg.467371>

1 Boğaziçi University, Department of Civil Engineering, İstanbul, Turkey - cem.tura@boun.edu.tr
<https://orcid.org/0000-0002-5745-6442>

2 Boğaziçi University, Department of Civil Engineering, İstanbul, Turkey - kutay.orakcal@boun.edu.tr
<https://orcid.org/0000-0001-5043-4024>

parameters (e.g., interstory drifts, story shear forces, story overturning moments, etc.) associated with the design of each individual tower.

Contrary to linear elastic analysis methods and strength based design used for regular structures, nonlinear response history analysis is required for tall buildings within the performance based design framework. Nevertheless, in real-life practice, due to time restrictions on project schedules, analysis of multiple towers using a combined structural model is typically not employed, and interaction effects between multiple towers are simply neglected, since computational demand for nonlinear response history analyses of multiple-tower models is significantly high. However, diaphragm forces developing in the podium floors of such structures is not an issue that can be disregarded in design.

Multiple towers on common podium buildings were not prevalent up to recent years since such structures were designed using seismic joints, forcing the response of the towers to be independent of each other. Therefore, although there is a scarce amount of relevant research in the literature, analysis of multiple towers on a common base is a subject that is not yet adequately investigated. One of the few studies that focus on multiple towers on common base is conducted by Qi and Chen [1]. Dynamic behavior of two towers connected with a typical podium structure is investigated through a parametric study. Towers and podium levels are modeled linear elastically using a lumped mass and equivalent stiffness approach. A simplified three degree of freedom (DOF) system is analyzed under a “constant” acceleration response spectrum, considering variation in mass and stiffness characteristics. This early study identifies the interaction effects between the towers to the seismic response of each, considering linear elastic forces only. However, this study does not include investigation of diaphragm effects at the connecting podium levels. In a more recent study by Behnamfar et al. [2], the importance of interaction effects between the two structures with various dynamic properties are addressed. A formulation is developed for simple multi degree of freedom systems to examine the severity of interaction forces on each structure. Linear springs are suggested for analysis using separate models for each tower. However, these linear springs are intended to represent only the kinematic interaction between the towers and neglect kinetic interaction caused by inertial effects. In addition, defining stiffness values for these springs may be tedious in real projects with complex structural configurations, especially projects that contain more than two towers on a single podium. Furthermore, in high rise structures, kinetic (i.e., inertial) interaction caused by out-of-phase vibration of the towers can be more predominant compared to kinematic interaction. Although this study provides notable amount of information for structures where inertial interaction is not expected to significantly affect the structural response, it is not adequate for reliable seismic response analysis of structures with high rise towers and connecting podiums.

The dynamic interaction between the towers and its effect on the dynamic response of the overall structure and the diaphragm effects on the podium levels is an issue that is explicitly warned against in design guidelines [3, 4, 5]; however, extremely limited literature is available on the subject. There is a clear need for additional analytical studies on this topic, which focus on the nonlinear response of real-life structural systems. As well, considering computational limitations, there is also a need for development of more practical approaches to be used for analysis and design of such structures.

Therefore, in this study, a practical approach is sought to evaluate the seismic response of structures incorporating multiple towers on a single podium, with emphasis on assessment of diaphragm effects at the podium levels. The main motivation is to assess whether critical response quantities for the towers and the podium floors can be approximately obtained within less computation time, by analyzing the towers separately with different assumptions for the end restraints, instead of using a combined model for analysis of the multiple tower structure.

Within the scope of this work, linear and nonlinear models of a hypothetical structure with two towers on a common podium are generated. The structure is analyzed using single-tower and combined double-tower models. The combined double model incorporates the entire structure including the towers, as well as the connecting podium and basement levels. The single models consist of a single individual tower, together with the corresponding half of the podium and basement floors, with different kinematic boundary conditions defined at the interface.

2. METHODOLOGY

2.1. Building Properties

The hypothetical reinforced concrete structure investigated in this study consists of two towers with 44 stories above and five stories below ground level. With 3.2 m typical height for each story, total height of the structure is 156.8 m and clear heights of the towers are 140.8 m. An identical structural system for both towers consist of a core wall system connected with coupling beams, T-shaped walls, outrigger beams (connecting core walls to perimeter walls), and perimeter frames along all four edges. The two towers are connected to each other by four podium floors above ground level, as well as five basement floors surrounded by perimeter walls (Figure 1). Architectural properties of the building are assumed such that the basement floors are utilized as parking garages, podium floors are utilized as commercial zones, and towers are utilized as residential buildings. Based on strength based design of the structure compliant with Turkish Building Earthquake Code 2018 (TBEC2018) [6], cross-sectional dimensions of the structural members are obtained as presented in Table 1.

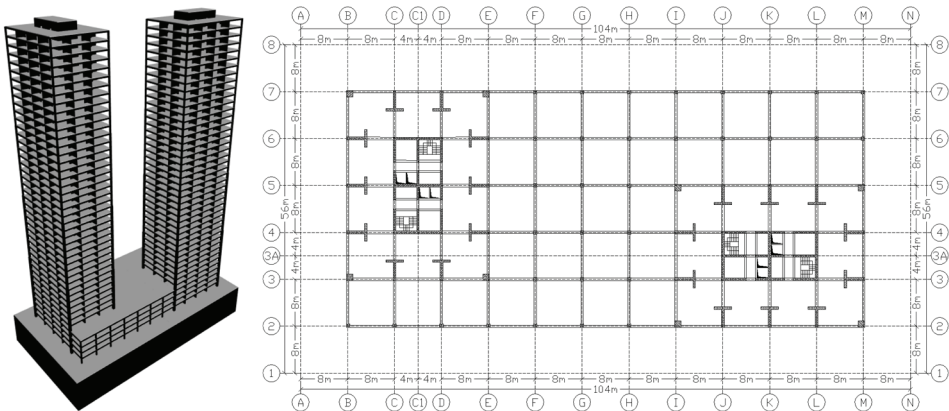


Figure 1 - 3D view of the structure and typical plan view for connected podium floors.

Table 1 - Cross-sectional dimensions of the structural members.

	-16.00m +00.00m	+00.00m +12.80m	+12.80m +35.20m	+35.20m +67.20m	+67.20m +102.4m	+102.4m +137.6m
Core Wall Web (restrained at both ends)	500mm				400mm	
Core Wall Flange (restrained at one end)	400mm				300mm	
T-Wall Web	500mm				400mm	
T-Wall Flange	400mm				300mm	
Basement Perimeter Walls	400mm	N/A				
Tower Columns	1200/1200mm	1100/1100mm	900/900mm	800/800mm	700/700mm	600/600mm
Podium Columns	800/800mm	600/600mm	N/A			
Coupling Beams	400/750mm				300/750mm	
Outrigger Beams	500/700mm				400/700mm	
Perimeter Frame Beams	400/600mm					
Podium Beams	400/600mm		N/A			
Slab	200mm					

2.2. Interaction Behavior

Interaction effects between the two towers can be classified into kinematic interaction and kinetic (inertial) interaction. Kinematic interaction is the effect of a tower to nearby towers due to its lateral stiffness properties. This type of interaction can be modeled using linear springs with constant stiffness. Second type of interaction is inertial interaction, which is related to the relative (in-phase, out-of-phase, or in-between) vibration of the towers due to their respective inertial properties. This type of interaction cannot be simply modeled using linear springs with stiffness values obtained from static analysis, since stiffness of the springs would change depending on relative displacements (deformed shape) of the towers at the podium levels.

The scope of this analytical study comprises evaluating the aforementioned dynamic interaction effects on the seismic response of a representative multiple-tower structure, in terms of the in-plane axial and shear forces developing in the podium and basement level diaphragms, as well as the seismic response demands of the individual towers, using a combined structural model of the multi-tower system and employing both linear and nonlinear modeling and analysis methods. Analysis results obtained using the combined model are also compared to simplified upper bound and lower bound modeling and analysis approaches, where the lower bound approach simply neglects the interaction between the towers and the upper bound approach can be interpreted to represent the interaction to the full extent. Prior to conducting analyses using a double (combined two-tower) model, single (one-tower) models are generated, by cutting the double model along the centerline of the podium structure between the two towers (Figure 2). For the case when the response of two towers completely out of phase, fixed supports are assigned to the joints where double model is cut. With this approach, the single models are analyzed assuming that there is an identical tower with completely symmetric response on other side of the cutting plane. On the other hand, for the case when response of two towers are completely in phase, no horizontal restraint (roller supports) are assigned to the joints where the double model is cut. Using this approach, the single models are analyzed assuming that there is an identical adjacent tower, with an identical response on other side of the cutting plane. Depending on these extreme assumptions, linear and nonlinear analysis results obtained using single fixed and single free models for both towers are compared with analysis results of the combined double tower model.

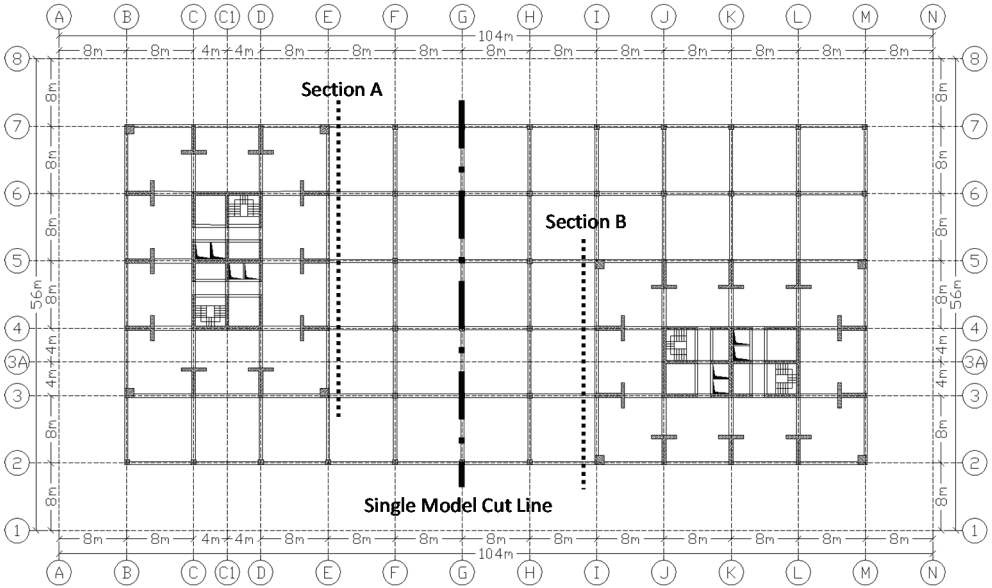


Figure 2 - Section cut and single model cut line locations.

2.3. Linear Elastic Modeling

Linear elastic models of the structure are generated using CSI ETABS [7] software for linear analyses. For linear modeling, concrete elastic modulus is defined as defined in Requirements for Design and Construction of Reinforced Concrete Structures (TS500) [8]. In design of this structure, C50 concrete class and B420C reinforcing steel grade are used, with characteristic compressive strength of $f_{ck}=50$ MPa and yield strength $f_{yk}=420$ MPa, respectively. Effective rigidity of structural members, masses and damping characteristics are defined according to TBEC2018. Modeling assumptions used are compliant with the criteria in TBEC2018. Loads corresponding to different architectural utilization properties are defined according to Design Loads for Buildings (TS 498) [9]. Natural vibration periods and corresponding modal mass participation ratios of the structure obtained using free vibration analysis are provided in Table 2 for the model configurations generated. Based on free vibration analysis of the double model, fundamental mode shapes of the towers are also presented in Figure 3. To satisfy the total mass participation of 95% in each direction requirement defined in TBEC2018, first 120 modes of the structure are included in analyses.

Table 2 - Fundamental vibration periods and corresponding mass participation ratios of the towers for single fixed, double, and single free models.

		Tower A			Tower B		
		Fixed	Double	Free	Fixed	Double	Free
X Direction	Period	4.88s	5.20s	5.44s	3.96s	4.08s	4.29s
	Mass Participation	43.7%	31.6%	48.6%	42.7%	14.9%	47.1%
Y Direction	Period	4.08s	4.29s	4.33s	5.12s	5.41s	5.48s
	Mass Participation	46.7%	21.5%	50.5%	43.5%	25.9%	46.8%

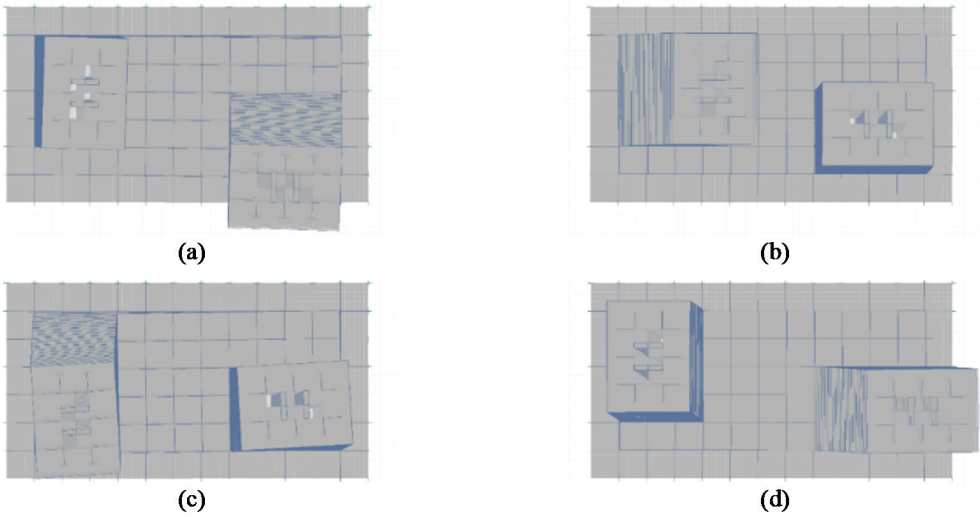


Figure 3 - Mode shapes for fundamental periods (a) TBY, (b) TAX, (c) TAY, (d) TBX.

2.4. Nonlinear Modeling

Nonlinear models of the structure (Figure 4) are generated using the commonly-used software Perform3D [10]. Methods, assumptions, and criteria used in modeling and analysis of the structure are compliant with specifications in TBEC2018, and recommendations in LATBSDC2015 [4] and ASCE41-13 [11]. Based on the state-of-the-art design codes and guidelines, nonlinear flexural behavior of beams and columns are modeled using the so-called lumped plasticity (plastic hinge) approach (Figure 5), utilizing ASCE41-13 backbone relationships, whereas nonlinear flexural behavior of the structural walls is modeled using the distributed plasticity (fiber modeling) approach (Figure 6). Floor slabs at the podium levels and the basement walls, which are expected to remain linear elastic under seismic effects, are included in the nonlinear model using linear elastic material properties. Floor slabs of the tower structures are not included in the model, and their in-plane stiffness is idealized using a rigid diaphragm constraint in the model. For nonlinear modeling, the expected compressive strength of concrete is defined as $f_{ce} = 65$ MPa and the expected yield strength of reinforcing steel is defined as $f_{sye} = 504$ MPa, according to TBEC2018 and LATBSDC2015 specifications.

Majority of the hysteretic energy dissipation sources in the structure are considered in nonlinear analysis, by explicit modeling of the hysteretic behavior of the aforementioned structural members. Equivalent viscous damping characteristics of the structure (2.5% viscous damping ratio specified in TBEC2018 for tall buildings) is introduced in the model as 2.4% modal damping and 0.1% Rayleigh damping ratios, also for damping out higher vibration modes as suggested by Powell [12].

2.5. Analysis Methods

To evaluate the seismic response of the structure, various analysis methods that are commonly used in practice are adopted. These methods are linear modal time history analysis (LMTHA), response spectrum analysis (RSA) and nonlinear response history analysis (NLRHA).

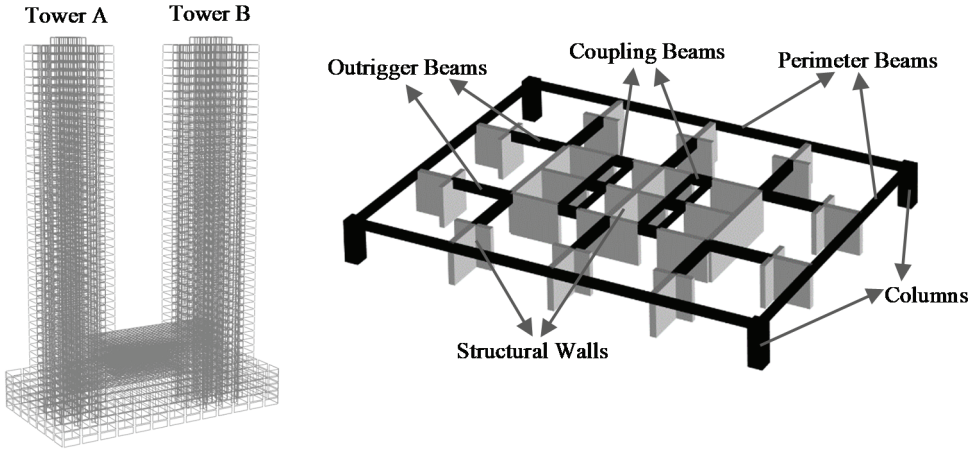


Figure 4 – Nonlinear double-tower model geometry and nonlinear structural elements.

2.6. Seismic Hazard Definition and Ground Motion Selection

The structure is analyzed under the DD1 and DD2 level earthquakes defined in TBEC2018, where DD1 (maximum credible earthquake) and DD2 (design level earthquake) levels corresponds to earthquake scenarios with probabilities of exceedance of 2% (2475 years recurrence period) and 10% (475 years recurrence period) in 50 years, respectively. Spectrum parameters at a hypothetical project site coordinates (40°58'39.1"N, 28°48'52.1"E) required to define the target spectrum are obtained from the Turkish Earthquake Hazard Map (TEHM) website [13] released by the Disaster and Emergency Management Presidency. Considering hazard levels at the site, distance between project site and closest active fault, as well as local soil conditions, design spectral acceleration coefficients are defined and design spectra are generated as shown in Figure 7 according to TBEC2018.

Ground motions are selected from the NGAWest2 Ground Motion Database [14] by matching the SRSS resultant acceleration spectra of the ground motion components with a target spectrum that is defined as 1.3 times the design spectrum defined in TBEC2018 (Figure 8) for the DD1 and DD2 level earthquakes. Details on ground motion selection and scaling, as well as detailed information on modeling and analysis of the investigated structure are presented by Tura [15].

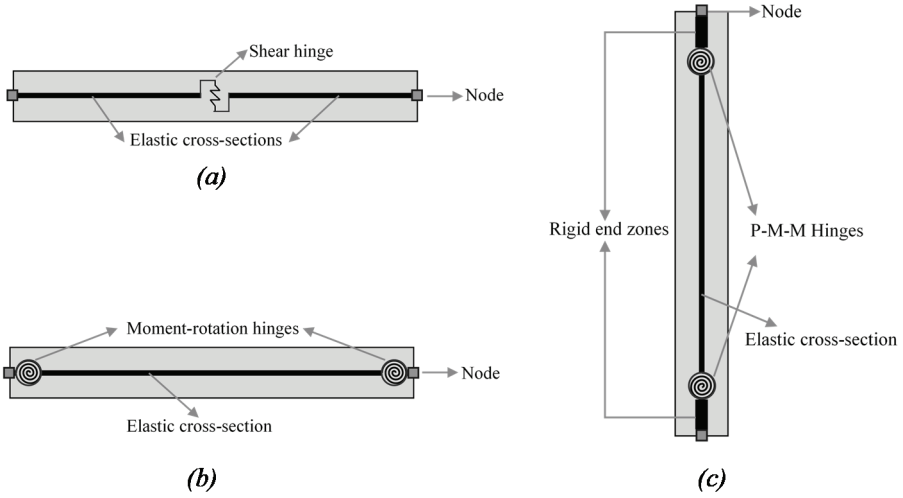


Figure 5 - Modeling of frame elements with lumped plasticity approach in Perform 3D; (a) coupling beams (b) outrigger and perimeter beams (c) columns.

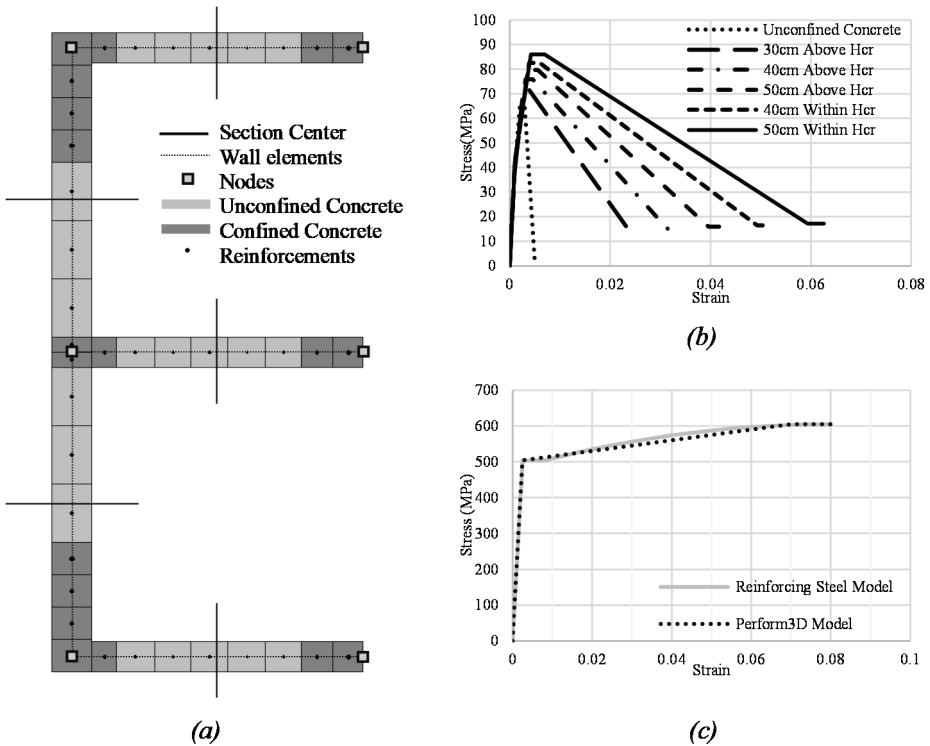


Figure 6 - Modeling of structural walls with distributed plasticity (fiber modeling) approach in Perform 3D; (a) cross-sectional view (b) unconfined and confined concrete stress-strain relationships (c) reinforcement stress-strain relationship.

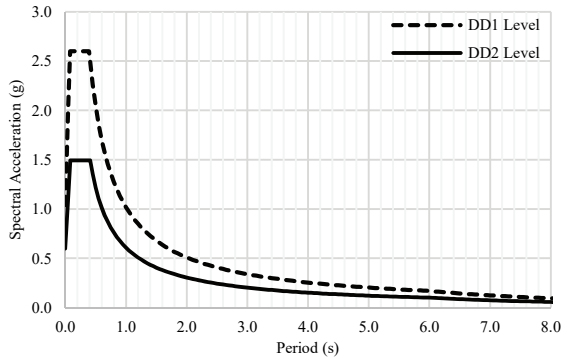


Figure 7 - Design spectra for DD1 and DD2 level earthquakes.

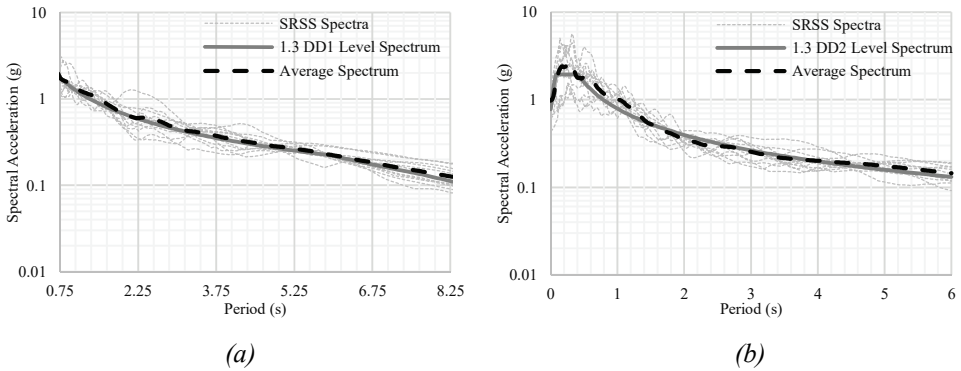


Figure 8 - SRSS acceleration spectra of selected ground motions for earthquake levels; (a) DD1 (b) DD2.

3. ANALYSIS RESULTS

In linear analyses, design spectrum of DD2 level (design level, i.e., 10% probability of exceedance in 50 years) seismicity (Figure 7) is used for RSA and 11 pairs of ground motion records selected for the target spectrum of DD2 level seismicity (Figure 8) are used for LMTHA. Furthermore, seismic demand is defined for linear analyses using a structural system behavior factor $R = 6$ for structural systems where all seismic demand is resisted by uncoupled structural walls according to TBEC2018. On the other hand, 11 pairs of ground motion records selected for the design spectrum corresponding to DD1 level (maximum credible, i.e., 2% probability of exceedance in 50 years) seismicity are used for NLRHA. In all response history analyses, total of 22 analyses are conducted, first by applying 11 ground motion record pairs, and secondly by reapplying the records at 90 degree rotated state. In all analyses, in-plane (diaphragm) tensile forces in X direction and in-plane (diaphragm) shear forces are obtained at section cuts defined adjacent to the tower edges (Figure 2). During evaluation of analysis results of linear analysis, earthquake effects are magnified using the over-strength factor $D = 2.5$, as is specified in TBEC2018.

3.1. Response Spectrum Analysis (RSA) Results

In plane distribution of resultant tensile forces (per unit slab length) in the floor diaphragm at +12.80 m elevation is presented in Figure 9 for RSA using the double-tower model. From the figure, stress concentration between the two towers due to interaction at the podium floors can be observed clearly. Resultant tensile force magnitudes in slab elements reach up to 600 kN/m at locations where stiff structural walls and floor slab are connected. In addition, due to beam action in the podium diaphragm, stress concentrations at upper and lower edges of the critical zone are noted. From a design perspective, when resultant tensile forces are compared with limit 330 kN/m corresponding to design tensile strength of concrete, it is clear that concrete cracks under tension and additional diaphragm reinforcement is required for code-compliant behavior.

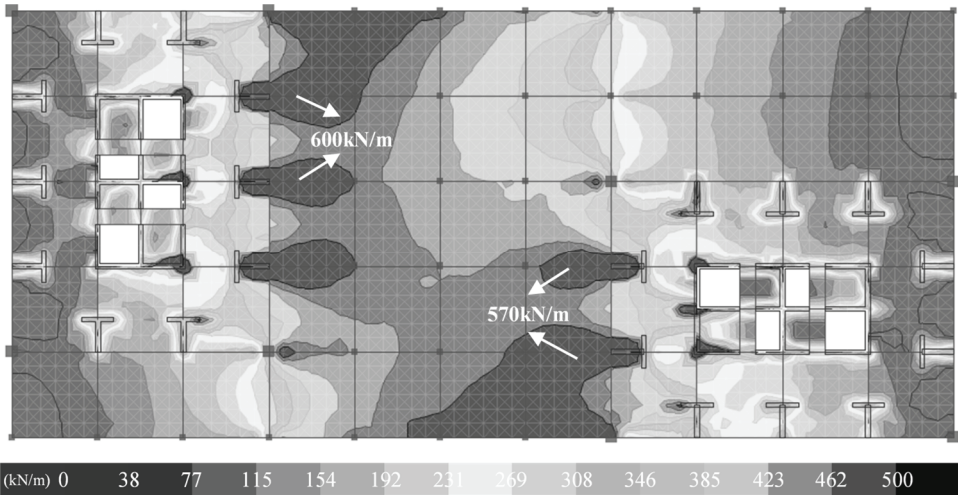


Figure 9 - Diaphragm tensile force distribution (in X direction) per unit length of slab at +12.80 m elevation of double model obtained from RSA.

Resultant tensile forces obtained from RSA of the double and single models, developing in the connected podium diaphragms are presented in Figure 10. As it is expected, interaction effects are much more critical at the uppermost diaphragm level compared to those at lower stories. When the resultant tensile forces at the section cuts are evaluated, it is clear that single models with fixed end restraints overestimate the in-plane axial forces at the connected podium slabs. According to section cut results obtained from RSA of the double model, average tensile stresses (averaged over the entire slab cross section) are calculated as 2.68 MPa for Section A and 2.75 MPa for Section B of the diaphragm, at +12.80 m elevation. In addition, axial loads on beams range between 800 kN and 1000 kN, with a total of 4420 kN at Section A and 3540 kN for Section B. Considering this distribution, additional diaphragm reinforcement can be designed as $\phi 16/300$ mm ($1340 \text{ mm}^2/\text{m}$) additional top and bottom reinforcement in slabs and $8\phi 20$ (2512 mm^2) skin (i.e., longitudinal web) reinforcement in beams at Section A, and $\phi 16/300$ mm ($1340 \text{ mm}^2/\text{m}$) additional top and bottom reinforcement in slabs and $8\phi 20$ (2512 mm^2) skin reinforcement in beams at Section B. Furthermore, when average stresses at lower podium levels are evaluated (1.36 MPa for Section A, 1.41 MPa for

Section B), it is noted that concrete at these levels does not crack under axial tension; therefore, no additional reinforcement in the slab or the beams is required.

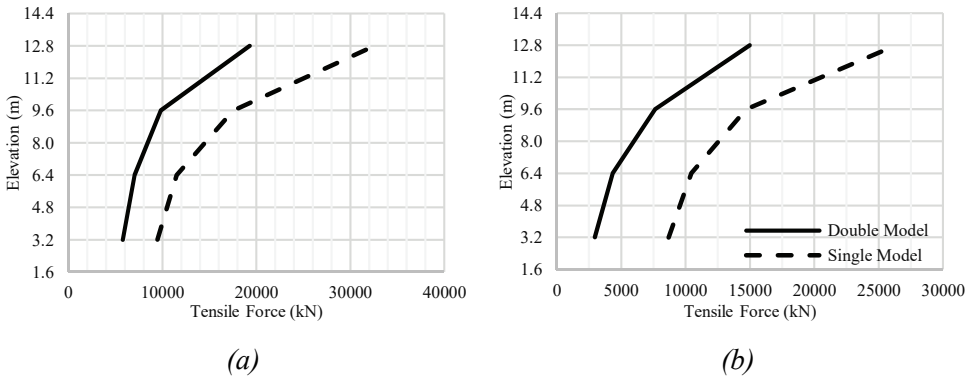


Figure 10 - Resultant tensile forces (in X direction) obtained from RSA at (a) Section A, (b) Section B.

On the other hand, if the single-fixed model analysis results are used in design, additional slab and beam reinforcement amounts calculated using the double model increase up to $\phi 16/200$ mm (2010 mm²/m) and $8\phi 26$ (4248 mm²) at Section A, and $\phi 16/175$ mm (2297 mm²/m) and $8\phi 26$ (4248 mm²) at Section B. Furthermore, according to the single-fixed model results, the diaphragm at +09.60 m elevation also cracks and it can be designed for $\phi 12/200$ mm (1130 mm²/m) additional reinforcement in the slabs and $6\phi 22$ (2280 mm²) skin (longitudinal web) reinforcement in beams at Section A, and $\phi 12/175$ mm (1291 mm²/m) additional reinforcement in the slabs and $8\phi 20$ (2512 mm²) skin reinforcement in the beams at Section B.

In-plane distribution of the resultant shear forces (per unit slab length) developing in the podium floor diaphragm at +12.80 m elevation is presented in Figure 11, based on RSA results using the double model. Resultant shear forces in the slab elements vary between 200 kN/m and 250 kN/m in the regions between the two towers. Comparing these magnitudes with a resultant shear force capacity 214 kN/m (corresponding to the concrete shear strength of 1.07 MPa), it is observed that diaphragm shear forces are as not critical as tensile forces for this structure. Furthermore, resultant shear forces in the connected diaphragms are presented in Figure 12 for RSA using double and single-fixed models. Similar to the tensile force distributions, total shear forces are highest at the uppermost connecting diaphragm, with magnitudes of 7046 kN at Section A and 5542 kN at Section B, and reduce throughout the lower stories down to 3785 kN for Section A and 2778 kN for Section B. Besides, resultant shear forces obtained using double and single-fixed models differ significantly, similarly to tensile force resultants. Therefore, if analysis results using the single-fixed model are used in design, average shear stress values increase up to 2.27 MPa for Section A and 2.41 MPa for Section B. Accordingly, the required amount of additional slab reinforcement for design increases up to 658 mm²/m for Section A and 734 mm²/m for Section B. Based on these demands, additional slab reinforcement can be designed as $\phi 12/350$ mm (646 mm²/m) top and bottom bars at Section A, and $\phi 12/300$ mm (753 mm²/m) top and bottom bars at Section B. Furthermore, according to section cut results of the fixed model under RSA,

average shear stresses in the diaphragm at +09.60 m elevation are calculated as 1.29 MPa at Section A and 1.35 MPa at Section B. Since these average stress levels are very close to the concrete design shear strength of 1.07 MPa, the required amount of additional reinforcement can also be considered to be negligible for design purposes.

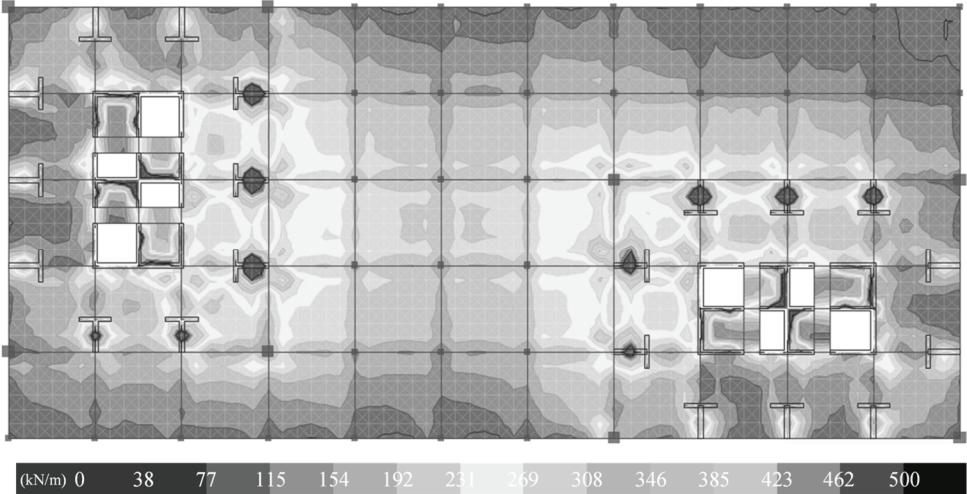


Figure 11 - Diaphragm shear force distribution per unit length of slab at +12.80 m elevation of double model obtained from RSA.

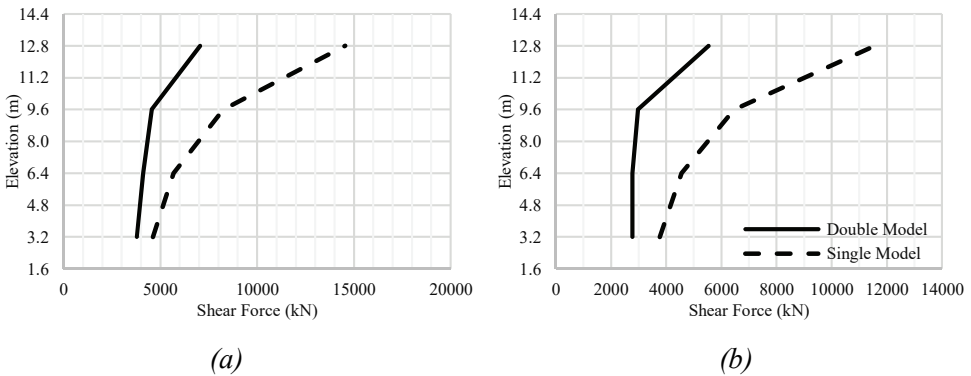


Figure 12 - Resultant diaphragm shear forces obtained from RSA at (a) Section A, (b) Section B.

3.2. Linear Modal Time History Analysis (LMTHA) Results

Distribution of resultant tensile forces in the floor diaphragm at +12.80 m elevation is presented in Figure 13 for LMTHA of the double model under the DD2 level earthquake. When LMTHA and RSA distributions are compared, it is observed that LMTHA gives

similar resultant tensile force magnitudes and distributions compared to RSA results. The only difference noted is marginally smaller magnitudes at critical regions of the diaphragm.

Resultant tensile forces in the connected podium floors, obtained from LMTHA of the structure using the double and single-fixed models, is presented in Figure 14. For consistency with RSA results, mean of 22 analysis results are presented in the table and figure. Similar to RSA, analysis results of the single-fixed model overestimate the double model results. Based on the average of 22 analyses, maximum resultant tensile force values obtained in the first connecting diaphragm are 18024 kN at Section A and 14322 kN at Section B. These resultants corresponds to average tensile stresses of 2.50 MPa at Section A and 2.63 MPa at Section B. Since these stress levels are close to results of RSA, an identical reinforcement design is applicable to resist the diaphragm forces.

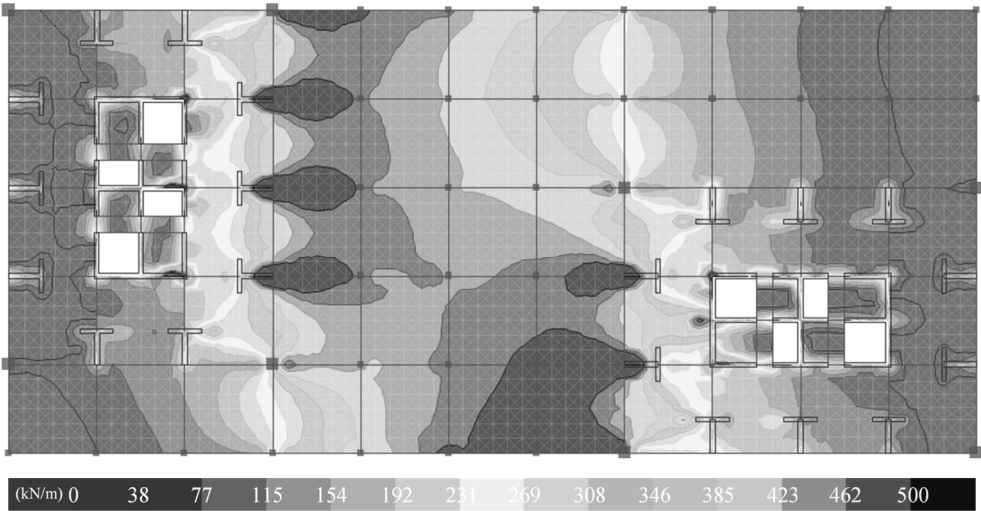


Figure 13 - Diaphragm tensile force distribution (in X direction) per unit length of slab at +12.80 m elevation of double model obtained from LMTHA.

In-plane distribution of resultant shear forces in the floor diaphragm at +12.80 m elevation is presented in Figure 15 for LMTHA using the double model. Similar to tensile forces, distribution of resultant shear forces are also similar to RSA results. As was the case in RSA, resultant shear forces (per unit length) in the slabs vary between 200 kN/m and 250 kN/m in the region between the two towers.

Resultant shear forces along the connected podium floors are presented in Figure 16 for LMTHA using single-fixed and double models. Similar to RSA, analysis results obtained using the single-fixed model overestimate the double model results. According to average of 22 analyses, maximum resultant shear forces (per unit slab length) developing in the topmost connecting diaphragm are 5359 kN at Section A and 4324 kN at Section B. These resultants correspond to average shear stresses of 0.84 MPa at Section A and 0.90 MPa at Section B. Since these shear stress levels do not exceed the concrete design shear strength of 1.07 MPa, no additional diaphragm shear reinforcement is required.

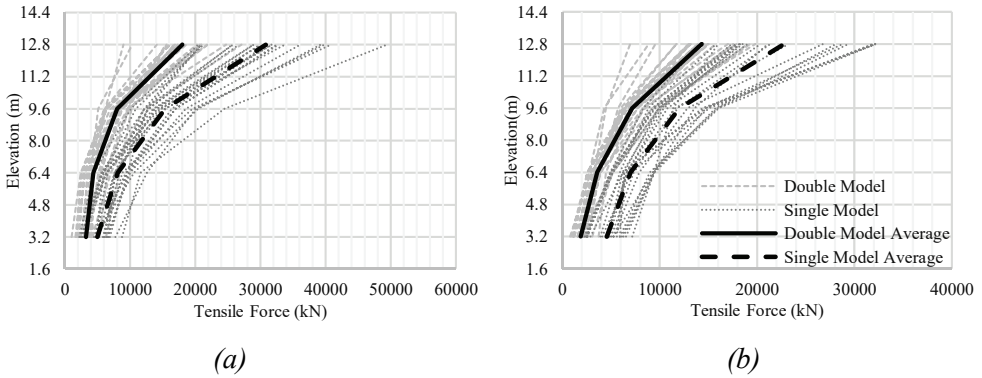


Figure 14 - Resultant tensile forces (in X direction) obtained from LMTHA at (a) Section A, (b) Section B.

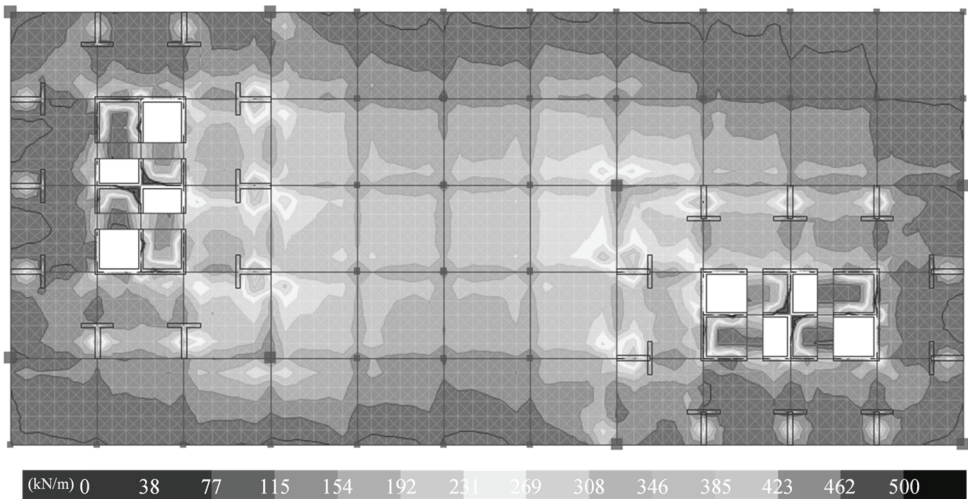


Figure 15 - Diaphragm shear force distribution per unit length of slab at +12.80 m elevation of double model obtained from LMTHA.

On the other hand, if single-fixed model analysis results are used in design, average shear stresses increase up to 2.27 MPa at Section A and 2.18 MPa at Section B. Since these stresses exceed the design shear strength of concrete 1.07 MPa, the required amount of additional slab reinforcement increases up to 658 mm²/m at Section A and 608 mm²/m at Section B at this level. According to these amounts, additional slab reinforcement can be designed as $\phi 12/350$ mm (646 mm²/m) top and bottom bars at Section A, and $\phi 12/350$ mm (646 mm²/m) top and bottom bars at Section B. In addition, according to section cut results of the fixed model under LMTHA, average shear stresses in the diaphragm of +09.60 m elevation are calculated as 1.34 MPa at Section A and 1.29 MPa at Section B. Since these stress levels are very close to the concrete design shear strength of 1.07 MPa, the required amount of additional slab reinforcement is negligible in design.

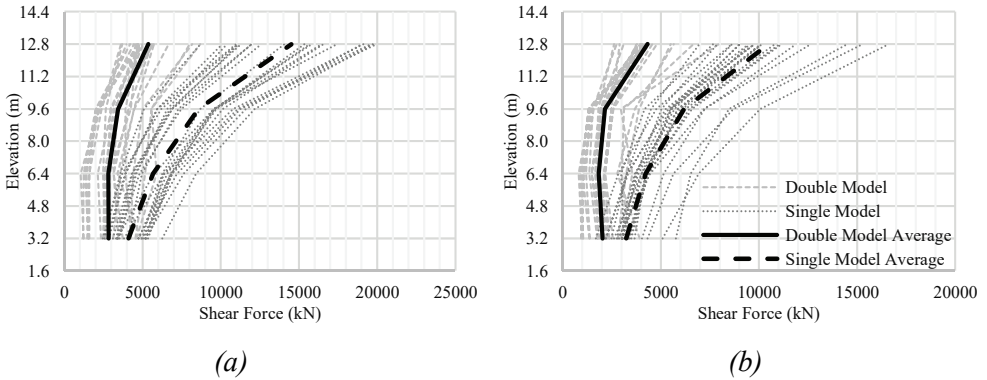


Figure 16 - Resultant diaphragm shear forces obtained from LMTHA at (a) Section A, (b) Section B.

In the following figures, comparison of resultant tensile and shear forces obtained from RSA and LMTHA of the single-fixed and double models, throughout the connected podium floors are presented. According to Figure 17, LMTHA consistently gives smaller tensile force values with respect to RSA. Resultant tensile forces at critical sections are very close to each other at the topmost connecting diaphragm, except for the single model results obtained for Tower B. Furthermore, differences in results of the two analysis methods are more significant at lower diaphragm levels. Similarly, according to Figure 18, diaphragm shear force resultants obtained by LMTHA are generally smaller than RSA results. The only exception is the fixed model results for the section cut at +09.60 m elevation of Tower A. At this section, the result of LMTHA is barely higher than the RSA result.

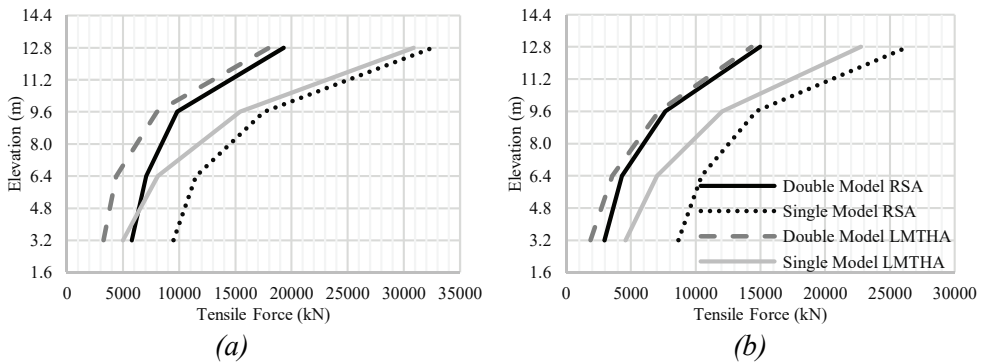


Figure 17 - Comparison of resultant diaphragm tensile forces (in X direction) obtained from LMTHA and RSA at (a) Section A, (b) Section B.

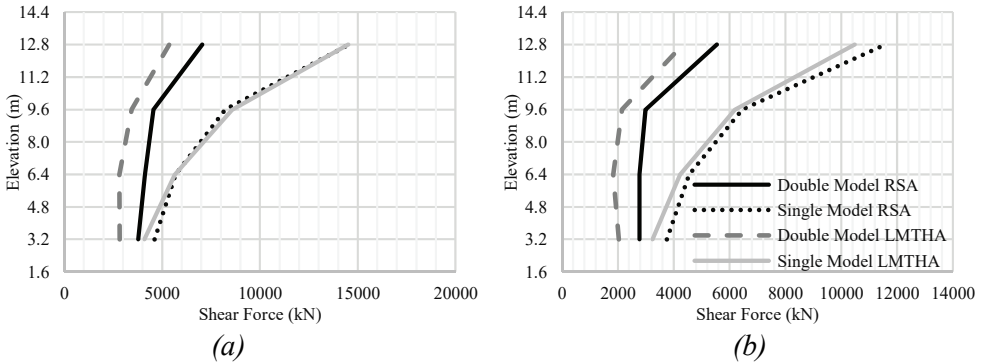


Figure 18 - Comparison of resultant diaphragm shear forces obtained from LMTHA and RSA at (a) Section A, (b) Section B.

3.3. Nonlinear Response History Analysis (NLRHA) Results

In this section, the diaphragm forces at the connecting podium levels are evaluated using a performance-based design approach, using NLRHA of the structure under the DD1 level earthquake (maximum credible earthquake, 2% probability of exceedance in 50 years), again using both double and single-fixed tower models. In the evaluation, diaphragm forces in the podium-level slabs and beams are considered as critical (i.e., non-ductile) response quantities and are assessed using a strength-based approach. Required amounts of diaphragm reinforcement obtained from NLRHA results to reach sufficient diaphragm strength are compared with reinforcement amounts obtained using linear analysis results under the design-level earthquake. Furthermore, seismic performance predictions obtained for Tower A using the double tower model under DD1 level ground motions are compared with predictions obtained using a single tower model, with both free and fixed end restraints at the connecting podium levels.

3.3.1. Podium Diaphragm Force Resultants

In order to facilitate convergence and reduce analysis time to a manageable level, podium diaphragms are modeled using shell elements with a relatively larger size in the nonlinear model of the structure. Although local distribution of the diaphragm forces is not captured since the diaphragms are more crudely-meshed, reliable values for diaphragm force resultants can still be obtained from the analyses. Because NLRHA of the double model required weeks of analysis time, analysis under different ground motion records were run in parallel, using separate models running on separate computers. For illustrative purposes, distribution of the diaphragm tension force (per unit length) developing in the topmost podium floor is illustrated in Figure 19, for a representative ground motion record referred to as RSN1762 [14] (used with a scaling factor of 3.326 in the analysis), which produces similar diaphragm force resultant magnitudes compared with the average of all 22 analyses. Differently from linear analysis results, due to the crude meshing, local stress concentrations in the slab at the structural wall connections are not recognizable. However, the overall distribution of the diaphragm tension forces is clearly shown in the figure. Tensile force concentrations between the two towers as well as at top and bottom edges of the connecting podium can be identified, similarly to the results of linear analysis.

Diaphragm tensile force resultants developing in the connected podium floors are presented in Figure 20, for the average of 22 NLRHA cases (corresponding to 22 ground motions). Compared to results of RSA and NLRHA, force resultant distribution along the podium floor elevations follows a similar pattern. However, there is 18% increase at Section A and 31% increase at Section B, in the total tensile force resultants at the floor with +12.80 m elevation, compared to RSA. This percent difference reaches upto 48% increase at Section A and 35% increase at Section B, when analysis results using the single-fixed models are considered.

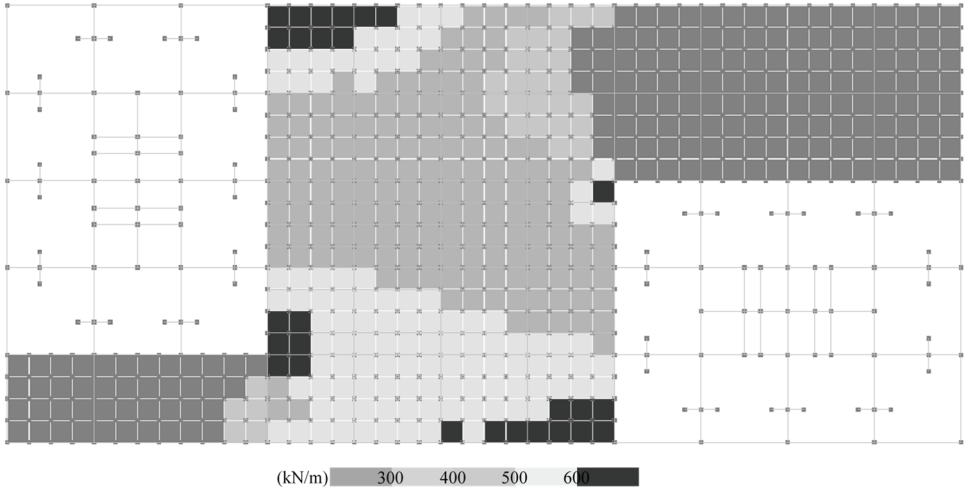


Figure 19 - Diaphragm tensile force distribution (in X direction) per unit length of slab at +12.80 m elevation of double model obtained from NLRHA under record RSN1762 [14].

Considering mean analysis results obtained using the double model, average tensile stresses developing at the topmost podium diaphragm are calculated as 3.17 MPa at Section A and 3.60 MPa at Section B. Comparing these stress levels with the expected tensile strength of concrete 2.82 MPa, it is deduced that concrete cracks in tension and additional reinforcement is required in these regions, similar to linear analysis results. Using the expected yield strength of reinforcement, total amounts of required slab reinforcement are calculated as 45339 mm² at Section A and 38813 mm² at Section B.

Furthermore, contribution of beams to the total tensile force resultant is obtained as 6762 kN at Section A and 5243 kN at Section B. Note that, percentages corresponding to contribution of beams to the total diaphragm tension force are 30% for Section A and 27% for Section B, whereas they were obtained as 23% for Section A and 24% for Section B from RSA. Taking into account all the information mentioned above, the required additional reinforcement can be designed as $\phi 14/300$ mm (1027 mm²/m) top and bottom bars in the slabs and 9 $\phi 20$ (2826 mm²) skin (i.e., longitudinal web) reinforcement in the beams at Section A, and $\phi 14/250$ mm (1232 mm²/m) top and bottom bars in slabs and 7 $\phi 22$ (2660 mm²) skin reinforcement in the beams at Section B. Average tensile stress levels at lower podium floors, which are 1.79 MPa at Section A and 1.88 MPa at Section B, are lower than the expected tensile strength of concrete. Therefore, no additional reinforcement is required to resist diaphragm tension at lower podium floors.

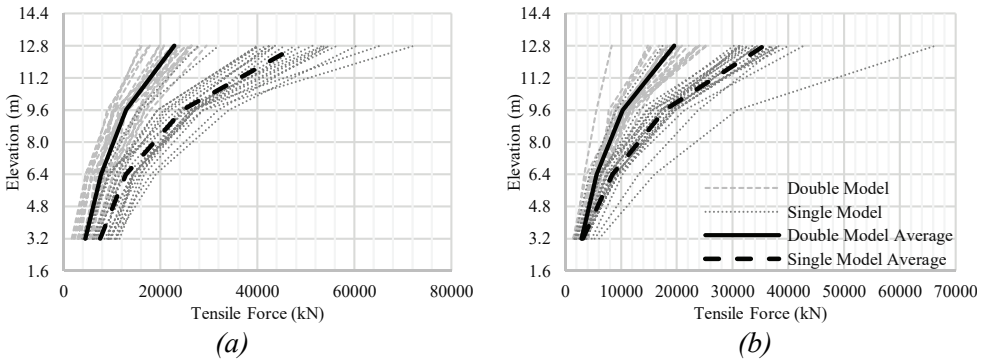


Figure 20 - Resultant tensile forces (in X direction) obtained from NLRHA at (a) Section A, (b) Section B.

On the other hand, when fixed model results are taken into account, average tensile stresses developing in the slabs at the topmost podium floor increase to 6.70 MPa at Section A and 6.82 MPa at Section B. According to these stresses, the required additional reinforcement can be designed as $\phi 18/250$ mm (2032 mm²/m) top and bottom bars in slabs, and 8 $\phi 30$ (5656 mm²) skin reinforcement in beams at Section A, and $\phi 20/300$ mm (2093 mm²/m) top and bottom bars in slabs and 8 $\phi 28$ (4928 mm²) skin reinforcement in beams at Section B. Additionally, average tensile stress levels at the podium floor of +09.60 m elevation increases to 3.41 MPa at Section A and 3.29 MPa at Section B. Therefore, concrete at this floor also cracks and additional tension reinforcement is required. Required additional reinforcement at this elevation can be designed as $\phi 14/300$ mm (1027 mm²/m) top and bottom bars in slabs and 8 $\phi 22$ (3040 mm²) skin (i.e., longitudinal web) reinforcement in beams at Section A, and $\phi 14/300$ mm (1027 mm²/m) top and bottom bars in slabs and 8 $\phi 20$ (2512 mm²) skin reinforcement in beams at Section B.

In plane distribution of diaphragm shear forces (per unit length) in the podium floor slab at +12.80 m elevation is presented in Figure 21 for NLRHA of the double model under the RSN1762_0 [14] ground motion record (scaled with a factor of 3.326). Similarly to diaphragm tensile forces, despite crude meshing, diaphragm shear effects are clearly reflected in the analysis results. The in-plane shear force distribution is similar to linear analysis results.

Resultant diaphragm shear forces along the connected podium floors are presented in Figure 22, as average of the 22 analysis cases used in NLRHA. Comparing results of RSA (Figure 12, under DD2 level earthquake) and NLRHA (Figure 22, under DD1 level earthquake), the distribution along the floors follows similar patterns in the single-fixed models, and slightly different patterns in the double models. In terms of magnitudes, there is a 91% increase at Section A and an 87% increase at Section B in the total diaphragm shear force acting on the podium floor with +12.80 m elevation in the double model, compared to RSA. This percent increase changes to 109% increase at Section A and 81% increase at Section B, when RSA and NLRHA results using fixed models are considered.

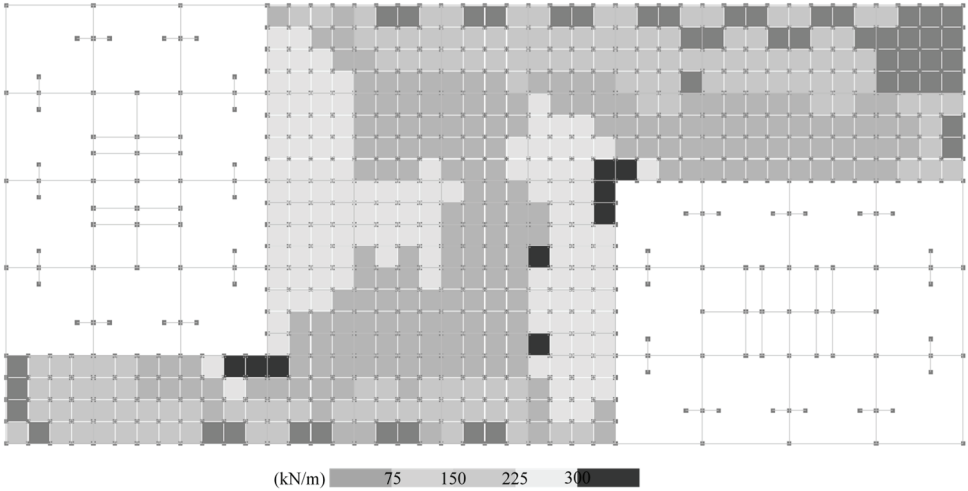


Figure 21 - Diaphragm shear force distribution per unit length of slab at +12.80 m elevation of double model obtained from NLRHA under RSN1762 [14] record.

Considering mean response quantities of double model, average diaphragm shear stress values at the topmost podium floor are calculated as 2.10 MPa at Section A and 2.16 MPa at Section B. Since these stress levels are very close to the concrete design shear strength 1.83 MPa, the required amounts of additional diaphragm shear reinforcement are negligible for design purposes. Furthermore, analysis results show that the contribution of beams to diaphragm shear forces is negligible, as is typical.

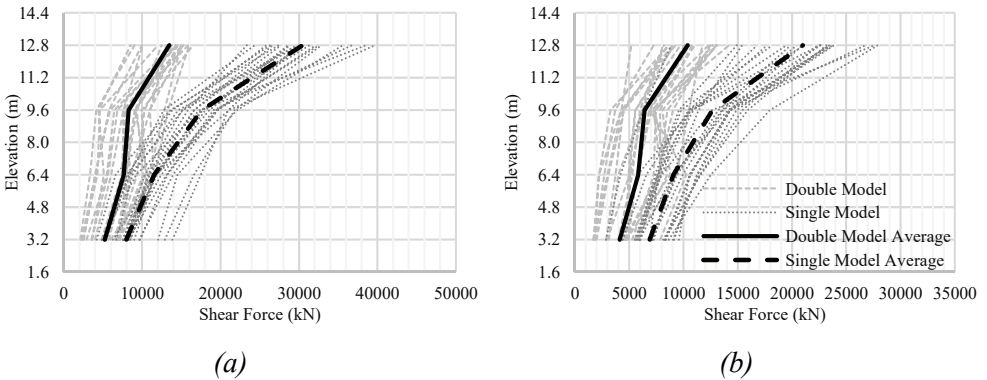


Figure 22 - Resultant shear forces obtained from NLRHA (a) Section A, (b) Section B.

On the other hand, if single-fixed model analysis results are considered in design, average diaphragm shear stress values at the topmost podium floor increase to 4.76 MPa at Section A and 4.37 MPa at Section B. Therefore, required amount of additional slab reinforcement increases up to 1163 mm²/m at Section A and 1008 mm²/m at Section B, at this elevation.

Corresponding reinforcement can be designed as $\phi 14/250$ mm ($1232 \text{ mm}^2/\text{m}$) additional top and bottom reinforcement at Section A and $\phi 14/300$ mm ($1027 \text{ mm}^2/\text{m}$) additional reinforcement at Section B. Again, diaphragm shear forces in the beams are negligible.

Additionally, based on section cut results from NLRHA of the fixed models, average diaphragm shear stresses at the floor with +09.60 m elevation are calculated as 2.75 MPa at Section A and 2.64 MPa at Section B. Considering these stress levels, the floor slab at this elevation can be designed using $\phi 10/400$ mm ($393 \text{ mm}^2/\text{m}$) additional top and bottom bars at Section A and $\phi 10/500$ mm ($314 \text{ mm}^2/\text{m}$) additional bars at Section B.

Finally, comparisons of diaphragm reinforcement required at critical sections, obtained using RSA (under DD2 level earthquake considering the code-prescribed load reduction factor and overstrength coefficient) and NLRHA (under DD1 level earthquake), are presented in Table 3 for Section A and Table 4 for Section B. According to the results listed in the tables, the amount of reinforcement required for design against diaphragm effects, obtained from RSA and NLRHA of the double model, are very close to each other. On the other hand, when fixed models are used for the analysis, the required amount diaphragm reinforcement obtained from NLRHA is moderately larger than that obtained using RSA.

It is also interesting to observe that the amount of diaphragm reinforcement obtained from NLRHA of the double model under the DD1 level earthquake, which is the most robust and reliable analysis approach, is less than the reinforcement amount obtained from RSA of the single fixed model under the DD2 level earthquake, which is the simplest analysis approach that can be used for diaphragm design. This happens mostly because the fixed model overestimates the diaphragm effects in the connecting podium floors, as previously discussed in detail, and also because the design based on NLRHA uses expected material strengths, rather than reduced design strength values for the materials. Overall, this is a comforting result, since it implies that diaphragm design of connecting podium floors based on simple RSA of a fixed single tower model under the design level earthquake can potentially satisfy the required performance criteria of the double tower structure under the maximum considered earthquake level

Table 3- Comparison of additional (diaphragm) reinforcement at Section A based on RSA (under DD2 level earthquake) and NLRHA (under DD1 level earthquake) results.

Section A			RSA (DD2 level EQ.)		NLRHA (DD1 level EQ.)	
			+12.80 m	+09.60 m	+12.80 m	+09.60 m
Double Model	Tension	Beams	2512 mm ²	0	2826 mm ²	0
		Slab	1340 mm ² /m	0	1027 mm ² /m	0
	Shear	Slab	0	0	0	0
Single-Fixed Model	Tension	Beams	4248 mm ²	2280 mm ²	5656 mm ²	3040 mm ²
		Slab	2010 mm ² /m	1130 mm ² /m	2032 mm ² /m	1027 mm ² /m
	Shear	Slab	646 mm ² /m	0	1232 mm ² /m	393 mm ² /m

Table 4 - Comparison of additional (diaphragm) reinforcement at Section B based on RSA (under DD2 level earthquake) and NLRHA (under DD1 level earthquake) results.

Section B			RSA (DD2 level EQ.)		NLRHA (DD1 level EQ.)	
			+12.80 m	+09.60 m	+12.80 m	+09.60 m
Double Model	Tension	Beams	2512 mm ²	0	2660 mm ²	0
		Slab	1340 mm ² /m	0	1232 mm ² /m	0
	Shear	Slab	0	0	0	0
Single-Fixed Model	Tension	Beams	4248 mm ²	2512 mm ²	4928 mm ²	2512 mm ²
		Slab	2297 mm ² /m	1291 mm ² /m	2533 mm ² /m	1027 mm ² /m
	Shear	Slab	753 mm ² /m	0	1027 mm ² /m	314 mm ² /m

3.3.2. Comparison of Single and Double Model Responses for Tower A

In this section, average analysis results obtained for important response quantities related to performance-based design of one of the two towers (Tower A), obtained using the double, single-fixed, and single-free models are compared (Figure 23). Comparisons of interstory drift ratios, beam plastic rotations, wall shear forces, and wall boundary longitudinal strains are presented in Figure 24 to Figure 28. As shown in the figures, it is observed that response quantities obtained using double tower model are typically underestimated by the single-fixed model (i.e., the single-tower model with fixed end restraints at the connecting podium levels), whereas the results of the single free model (i.e., the single-tower model with free end restraints) are much closer to those of the double-tower model. Overall, comparison with NLRHA results obtained using the double tower model show that the single-free model provides reliable results that are reasonably representative of the results of the comprehensive double-tower model, for important response quantities associated with the seismic design and performance of the individual tower structure.

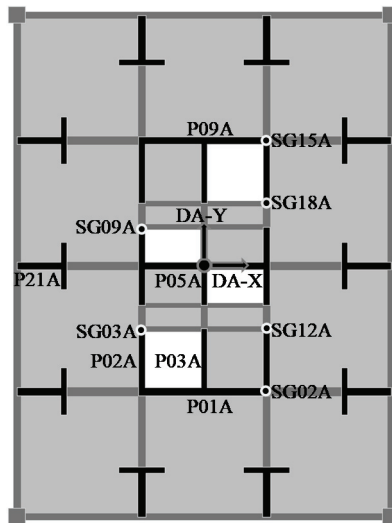


Figure 23 - NLRHA interstory drift ratio, structural wall shear force and strain control nodes for Tower A.

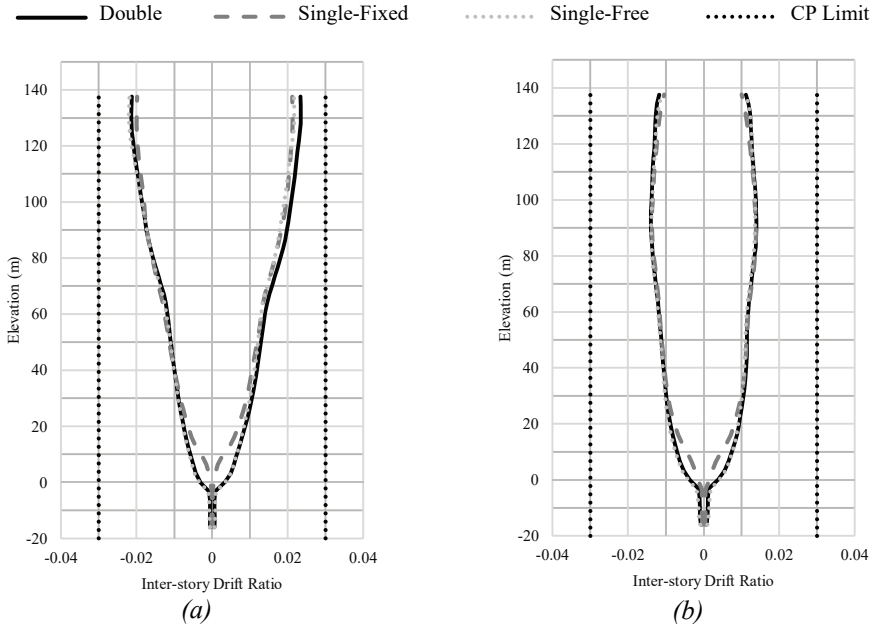


Figure 24 - Comparison of NLRHA interstory drift ratio distributions for double, single-fixed and single-free models of Tower A at (a) DA-X, (b) DA-Y.

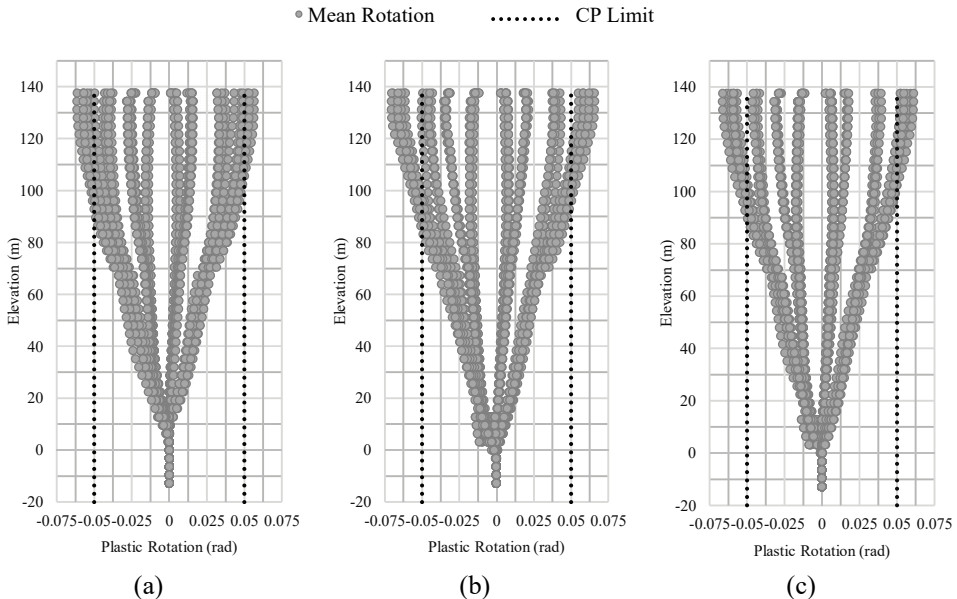


Figure 25 - Comparison of NLRHA outrigger and perimeter beams plastic rotations for (a) single-fixed, (b) single-free, (c) double models of Tower A.

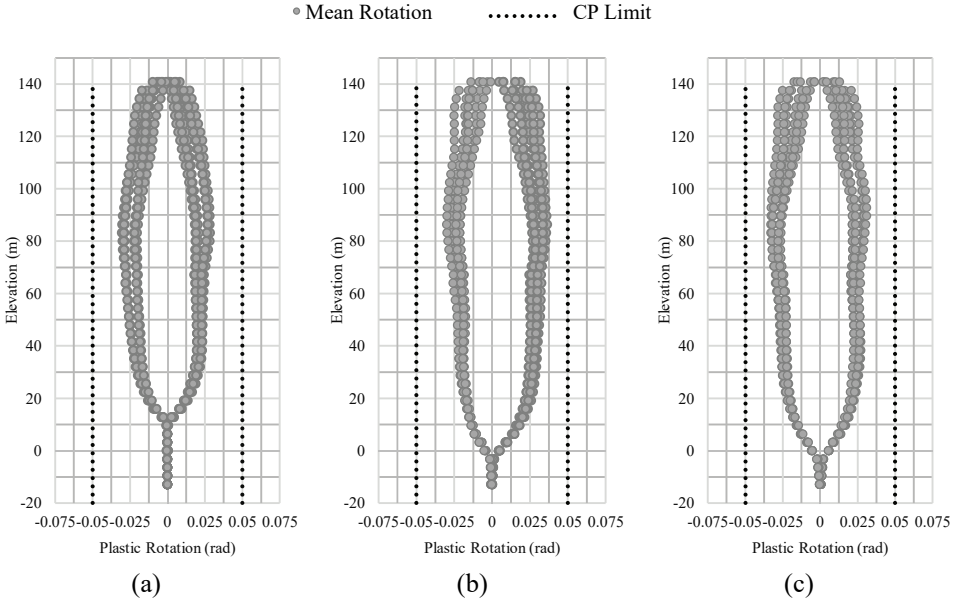


Figure 26 - Comparison of NLRHA coupling beam plastic rotations for (a) single-fixed, (b) single-free, (c) double models of Tower A.

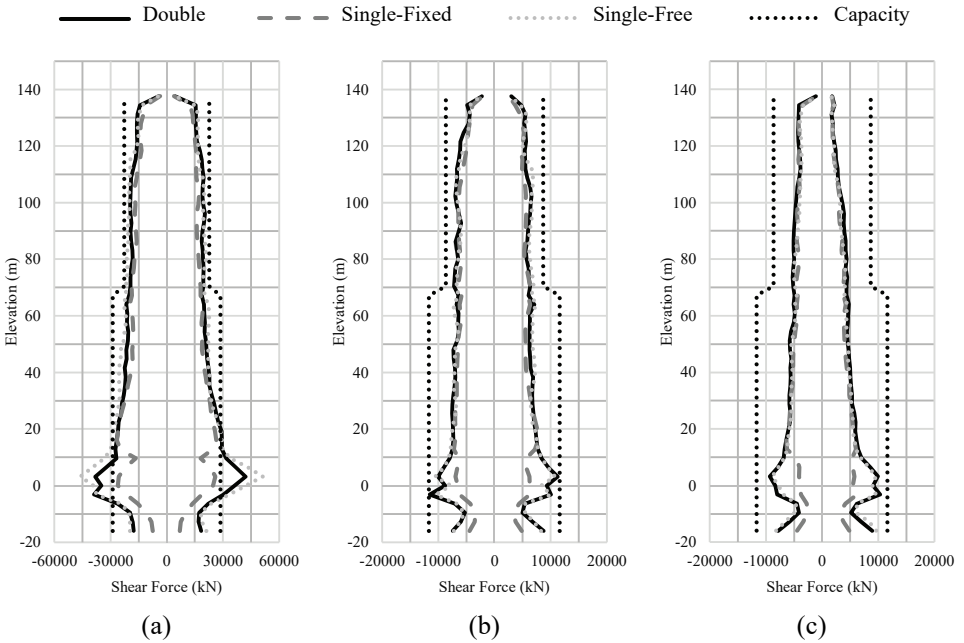


Figure 27 - Comparison of NLRHA structural wall shear force distributions for double, single-fixed and single-free models of Tower A at (a) P01A, (b) P02A, (c) P03A.

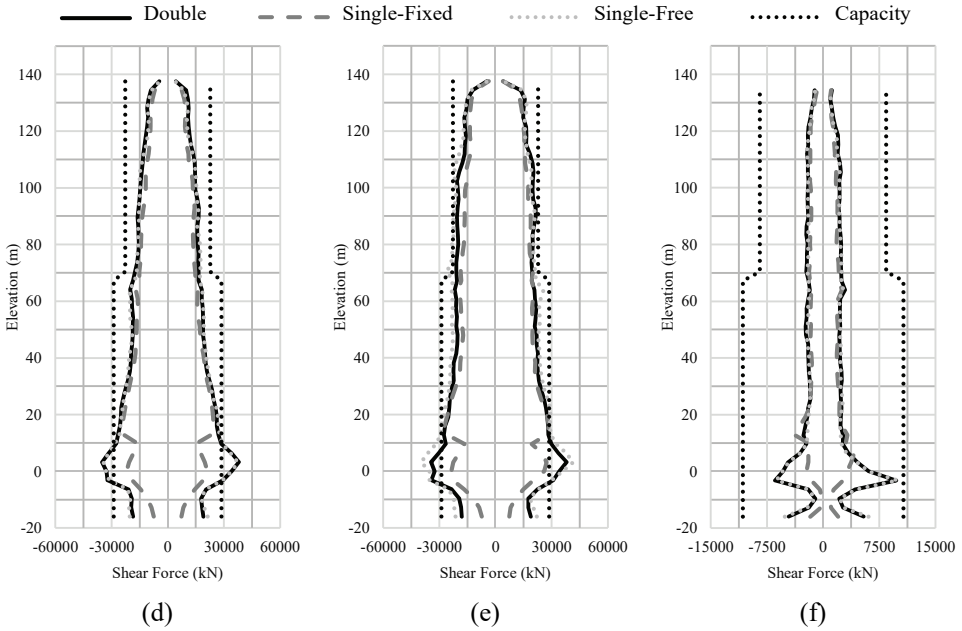


Figure 27 (continued) - Comparison of NLRHA structural wall shear force distributions for double, single-fixed and single-free models of Tower A at (d) P05A, (e) P09A, (f) P21A.

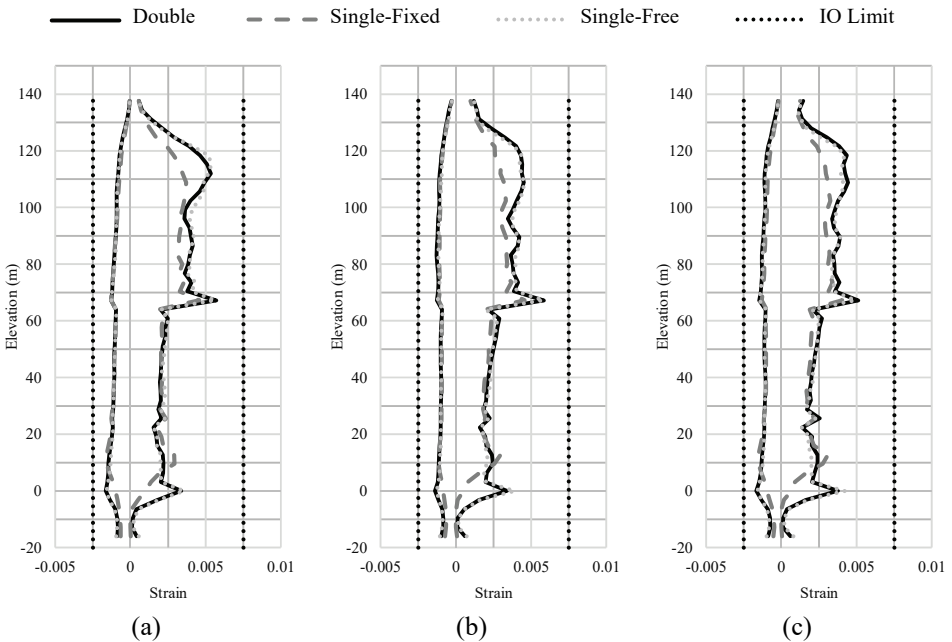


Figure 28 - Comparison of NLRHA strain distributions of structural walls for double, single-fixed and single-free models of Tower A at (a) SG02A, (b) SG03A, (c) SG09A.

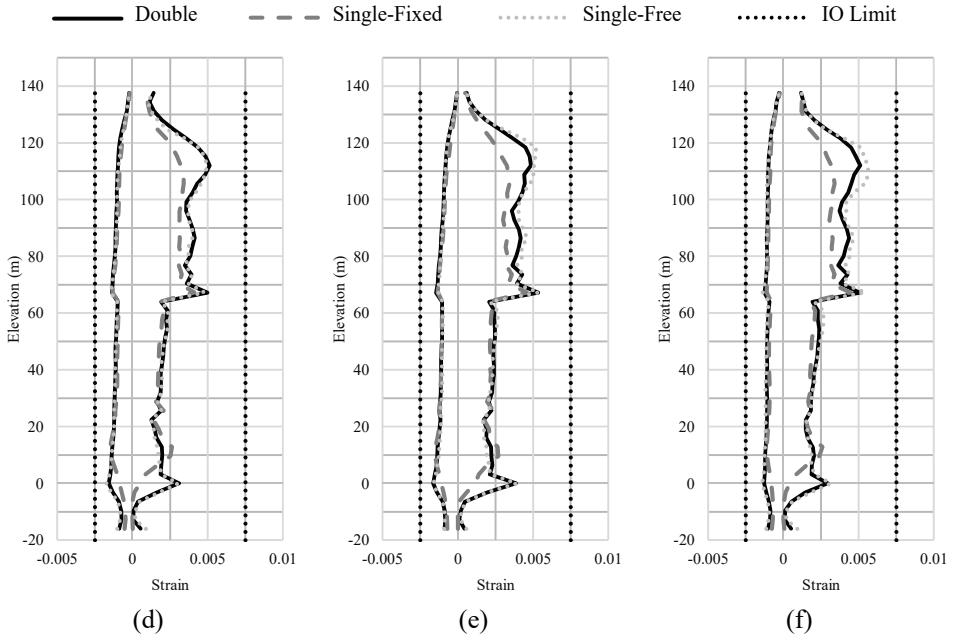


Figure 28 (continued) - Comparison of NLRHA strain distributions of structural walls for double, single-fixed and single-free models of Tower A at (d) SG12A, (e) SG15A, (f) SG18A.

4. CONCLUSIONS

Under the light of the analysis results obtained using different modeling approaches and analysis methods used in this study, the following conclusions can be drawn:

- When results of linear elastic analysis methods (RSA and LMTHA) conducted under the design level (DD2) earthquake effects using double (combined double tower) and single-fixed (single tower with fixed end restraints) model results are compared, it is observed that RSA provides diaphragm tensile force resultants that are only approximately 10% larger than LMTHA at the connected podium levels. The difference between results of the two analysis methods increase to 25% only for diaphragm shear forces obtained using the double model, yet these diaphragm shear forces are relatively small in magnitude.
- When linear elastic analysis results using the double and single-fixed models are compared, it is observed that the single-fixed model can provide diaphragm tension forces that are up to 75% higher than the double model results, independently from the analysis method used (RSA or LMTHA). However, this percent difference increases to more than 100%, when diaphragm shear forces are considered, also because the diaphragm shear force magnitudes are small.
- When results of NLRHA obtained using double and single-fixed models are compared, it is observed that the single-fixed model can provide diaphragm force resultants that are almost twice those calculated using the double model.

- NLRHA of the double model of the structure under the DD1 level (maximum credible) earthquake gives approximately 20-30% higher diaphragm tensile forces compared to RSA of the double model under the DD2 level (design level) earthquake. On the other hand, in case of diaphragm shear forces, NLRHA results obtained using the double model are almost twice those obtained from RSA at critical sections. Although NLRHA gives higher diaphragm forces, the total amount of required diaphragm reinforcement for tension is 5% to 15% less than RSA, since expected material strengths are used for design based on NLRHA results. Additionally, diaphragm shear forces obtained in both analyses do not exceed concrete shear strength limits, not necessitating any diaphragm shear reinforcement.
- Differently from the double model, when the single-fixed model is used in the analysis, NLRHA can produce 50% higher diaphragm tensile forces as compared to RSA. On the other hand, diaphragm shear forces from NLRHA are approximately twice those obtained by RSA, as observed in the double model. When required reinforcement amounts against diaphragm tension are compared, NLRHA results using the single-fixed model require approximately 10% larger amount of reinforcement, as compared to RHA of the single-fixed model.
- Interestingly, the amount of diaphragm reinforcement obtained from NLRHA of the double model under the DD1 level (maximum credible) earthquake, which is the most robust and reliable analysis approach, is less than the reinforcement amount obtained from RSA of the single-fixed model under the DD2 level (design level), which is the simplest analysis approach that can be used for diaphragm design. This happens mostly because the fixed model overestimates the diaphragm effects in the connecting podium floors, and also because the performance-based design based on NLRHA uses expected material strengths, rather than reduced design strength values for the materials.
- NLRHA results show that the single-free (single tower with free end restraints) model provides results for critical response quantities associated with the seismic performance of the individual tower structures (interstory drifts, wall strains, wall shear forces, beam plastic rotations, etc.) that are reasonably close to analysis results obtained using the double model.
- Generally, taking into consideration of analysis duration and modeling complexity, it is recommended to use single-tower models with free end restraints for design of the individual towers, and single-tower models with fixed end restraints for design of the podium slabs for in-plane axial load and shear forces, whenever comprehensive analyses using a combined multiple-tower model is not possible.

Notations

LMTHA Linear modal time history analysis

NLRHA Nonlinear response history analysis

RSA Response spectrum analysis

References

- [1] Qi Xiaoxuan, Chen Shuang, 1996, “Dynamic Behavior and Seismic Design of Structural Systems Having Multiple High-rise Towers on a Common Podium, Paper No. 1101”, Societat Mexicana De Ingenieria Sismica, Eleventh World Conference on Earthquake Engineering, Acapulco, Mexico, June’23-28, 1996, California.
- [2] Behnamfar F., Dorafshan S., Taheri A., Hashemi B. H., 2015, “A Method for Rapid Estimation of Dynamic Coupling and Spectral Responses of Connected Adjacent Structures”, The Structural Design of Tall and Special Buildings, Vol. 25, pp: 605-625.
- [3] Applied Technology Council, 2010, Modeling and Acceptance Criteria for Seismic Design and Analysis of Tall Buildings, ATC72-1, Pacific Earthquake Engineering Research Center, California.
- [4] Los Angeles Tall Buildings Structural Design Council, 2015, An Alternative Procedure for Seismic Analysis and Design of Tall Buildings Located in the Los Angeles Region, Los Angeles Tall Buildings Structural Design Council, California.
- [5] Pacific Earthquake Engineering Research Center, 2010, Guidelines for Performance-based Seismic Design of Tall Buildings, Report PEER-2010/05, Pacific Earthquake Engineering Research Center, University of California.
- [6] Turkish Building Earthquake Code, 2018, Specifications for Design of Buildings under Earthquake Action, Disaster and Emergency Management Presidency, Ankara.
- [7] ETABS Ultimate v16.1.0, 2017, Extended 3D Analysis of Building Structures, Computers and Structures, Inc., California, USA.
- [8] Turkish Standards Institute, 2000, Requirements for Design and Construction of Reinforced Concrete Structures, TS500, Turkish Standards Institute, Ankara Turkey.
- [9] Turkish Standards Institute, 1997, Design Loads for Buildings, TS498, Turkish Standards Institute, Ankara.
- [10] Computer and Structures, Inc., 2011, Perform 3D V6.0.0: Nonlinear Analysis and Performance Assessment for 3D Structures, California, USA.
- [11] ASCE/SEI Seismic Rehabilitation Committee, 2014, Seismic Evaluation and Retrofit of Existing Buildings, ASCE/SEI41-13, American Society of Civil Engineers, Reston, VA.
- [12] Powell, G. H., 2010, Modeling for Structural Analysis, Behavior and Basics, Computers and Structures Inc. Berkeley, California.
- [13] Disaster and Emergency Management Presidency, 2017, Turkish Earthquake Hazard Map <https://tdth.afad.gov.tr/>, accessed June 2017.
- [14] Pacific Earthquake Engineering Research Center, 2013, Next Generation Attenuation-West2, <http://ngawest2.berkeley.edu/>, accessed at June 2017.
- [15] Tura C., Earthquake Response Analysis of Multiple Towers on a Common Podium, M.S. Thesis, Boğaziçi University, 2017.

